Ultrafast Photonic Differentiator and Integrator Employing Integrated Silicon Microring or MZI

Jianji Dong, Shasha Liao, Aoling Zheng, and Ting Yang
Wuhan National Laboratory for Optoelectronics, School of Optical and Electronic Information
Huazhong University of Science and Technology, Wuhan 430074, China

(*Invited Paper*)

Abstract— Integrated microwave photonics is becoming one of the most promising topics due to the compact size, light weight, and low power consumption. In this paper, we review several schemes of ultrafast photonic differentiator and integrator employing integrated silicon microring or MZI.

1. INTRODUCTION

Photonic integrated circuits for photonic computing open up the possibility for the realization of ultrahigh-speed and ultra wide-band signal processing with compact size and low power consumption. As we all known, the two important parts of photonic computing are differential and integral. Photonic differentiator (DIFF) has wide applications in numerous fields such as pulse characterization, ultra-fast signal generation, and ultra-high-speed coding. And one of the most important application of integral is solve the differential equations, which can be used in many field of science and engineering, such as temperature diffusion processes, physical problems of motion subject to acceleration inputs and frictional forces, and the response of different resistor-capacitor circuits, etc..

DIFFs can be achieved by nonlinear effects of semiconductor optical amplifiers (SOAs) [1, 2], incoherent photonic processors [3] and highly nonlinear fibers [4]. The typical schemes to solve the differential equation have focused on two routes toward solving first-order all-optical differential equations. The first one requires an optical feedback loop [5, 6], while the second one is based on a Fabry-Perot (FP) resonance cavity with properly designed temporal impulse response [7]. Nevertheless, the configurations of these schemes are bulky and complex, involving either redundant loop [5, 6] or additional optical pump [6, 7].

In this review, we report several schemes of ultrafast photonic differentiator and integrator. In Section 2, we demonstrate a high-order DIFF and fractional-order DIFF based on Mach-Zehnder Interferometer (MZI) structure and demonstrate linear ODE solver with constant-coefficient tunable based on a single microring.

2. HIGH-ORDER PHOTONIC DIFFERENTIATOR USING SILICON MACH-ZEHNDER INTERFEROMETERS [8]

An Nth-order optical temporal differentiator provides the Nth-time derivative of the complex envelope of an input optical signal. It has been proved that the MZI structure has a good linear frequency response near the MZI resonant notch, which can implement the first order DIFF. Therefore, to achieve Nth-order differentiator, the MZI unit just needs to be cascaded by N times. We employ on-chip cascaded MZI structure for high-order DIFF. First we design and fabricate cascaded MZIs on commercial silicon-on-insulator (SOI) wafer. Fig. 1 shows the microscope image of our on-chip MZIs.

First, the laser wavelength is fixed at 1565.4 nm. And the BPG drives the two MZMs to generate a Gaussian pulse train with a pulsewidth of 18 ps, as shown in Fig. 2(a). When we employ the chips of MZI-1, MZI-2, and MZI-3, and fine tune the laser wavelength to align with the resonant notch, we measure the temporal waveforms of 1st order, 2nd order, and 3rd order DIFFs, respectively, which are shown in Figs. 2(b)–(d), respectively. It can be seen that the measured differentiated pulses fit well with the simulated pulses, except a small discrepancy in the pulse sidelobes, such as 2nd-order DIFF and 3rd-order DIFF. The deviation of the sidelobes may be caused by the finite bandwidth and the finite notch depth.

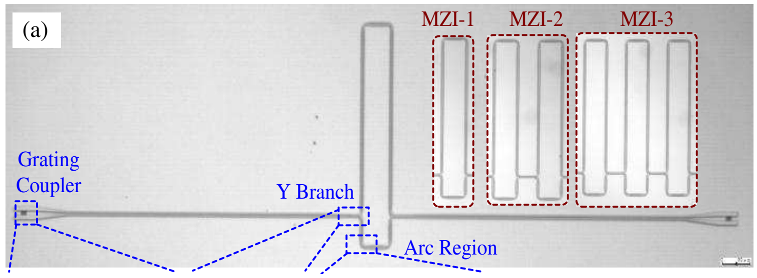

Figure 1: Microscope image of our on-chip MZIs, insets: photos of structures of MZI-1, MZI-2, and MZI-3.

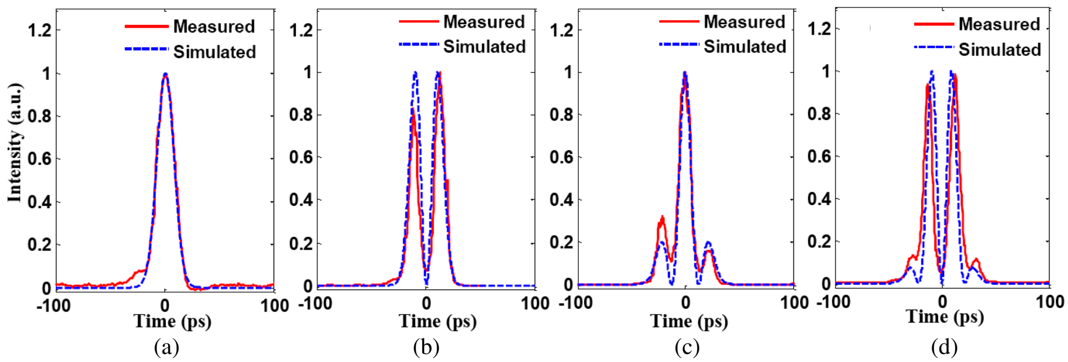

Figure 2: (a) input pulse, (b)–(d) temporal waveforms for 1st-, 2nd-, and 3rd-order DIFFs, respectively.

3. FRACTIONAL-ORDER DIFFERENTIATOR USING AN ELECTRICALLY TUNED SOI MACH-ZEHNDER INTERFEROMETER

From Eq. (2.1), we know that a MZI can play a role as a fractional-order differentiator if N is a fraction number and the power splitting ratio of two arms of MZI are not the same. So we fabricated an on-chip electrically tuned MZI to build a tunable fractional-order differentiator. Fig. 3 shows the micrographs of (a) total MZI structure, (b) coupling grating, (c) MMI, (d) *p*-*i*-*n* diode.

We change the voltage of the electrodes on the MZI, and fine tune the tunable laser diode wavelength to be aligned with the notch wavelength, the output differentiated waveforms are shown in Figs. 4(b)–(i). At the same time, the simulated waveforms of fractional-order differentiation are also shown, whose fractional orders are $N = 0.83, 0.85, 0.88, 0.93, 0.96, 0.98, 1.00, 1.03$, respectively. One can see there is a good agreement between the measured pulses and the ideal differentiators except a small discrepancy at the pulse notch.

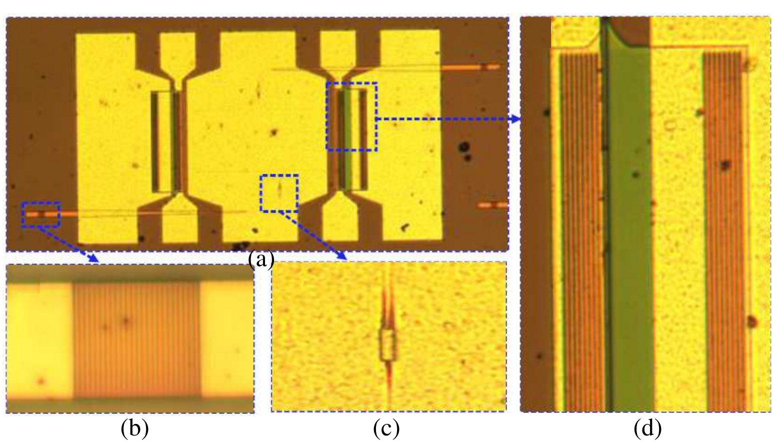

Figure 3: Micrographs of (a) MZI, (b) coupling grating, (c) MMI, (d) integrated *p*-*i*-*n* diode.

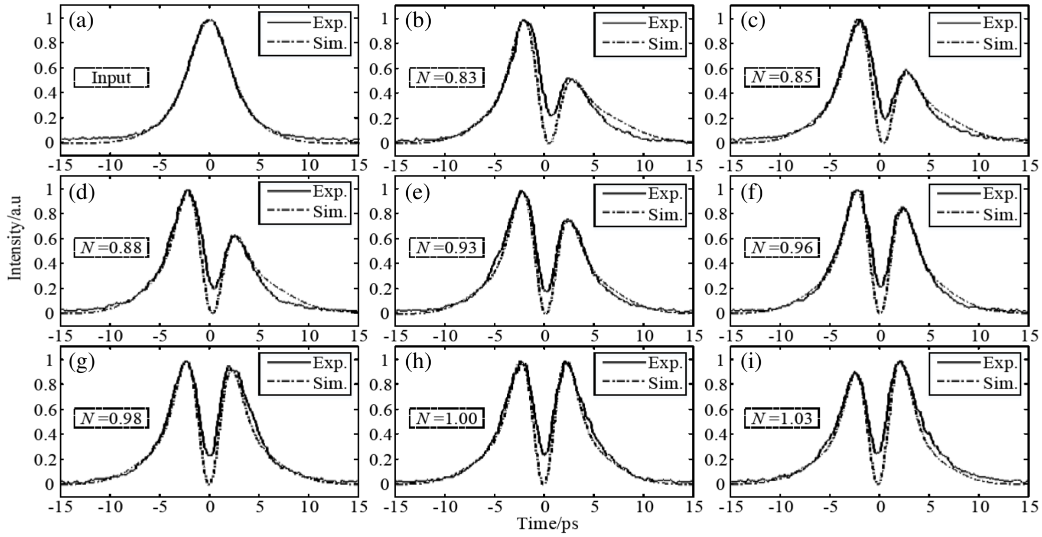

Figure 4: (a) An input Gaussian-like pulse with an FWHM of 5.4 ps, and the differentiated pulses at the different voltages corresponding to differentiation orders of (b) $N = 0.83$, (c) $N = 0.85$, (d) $N = 0.88$, (e) $N = 0.93$, (f) $N = 0.96$, (g) $N = 0.98$, (h) $N = 1.00$, (i) $N = 1.03$.

4. HIGH-ORDER ALL-OPTICAL DIFFERENTIAL EQUATION SOLVER BASED ON MICRORING RESONATORS

The common constant-coefficient first-order linear ODE can be expressed as:

$$\frac{dy(t)}{dt} + ky(t) = x(t) \tag{1}$$

where $x(t)$ represents the input signal, $y(t)$ is the equation solution (output signal) and k denotes a positive constant of an arbitrary value. We know that a silicon microring functions as a loss integrator, which has a similar transfer function to Eq. (1) at the drop port. Therefore, a single add-drop microring can be utilized to solve constant-coefficient first-order linear ODE. Similarly, cascading microrings can solve second-order linear ODE if two microring resonant peaks are matched.

The microrings we employed are two cascaded microrings fabricated on silicon-on-insulator (SOI) wafer with different radii ($R_1 = 100\,\mu\text{m}$, $R_2 = 130\,\mu\text{m}$) and Q factor ($Q_1 = 22038$, $Q_2 = 19045$), as illustrated in Fig. 5(a). The waveguide width and thickness of both straight and bending waveguide are 450 nm and 220nm, respectively, while the gap between them is 200 nm (Fig. 5(b)). Employing

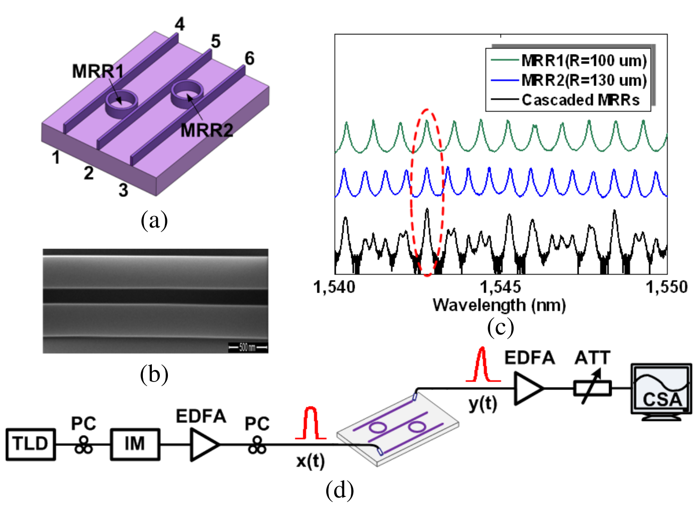

Figure 5: (a) Schematic of the cascaded microrings, (b) SEM picture of the coupling region between the ring and the straight waveguide, (c) measured spectra of each microring and the cascaded ones, (d) the experimental setup.

port 1 and 2, Microring 1 is used as a first-order all-optical ODE solver with the constant-coefficient $k_1 = 0.028/\text{ps}$; meanwhile Microring 2 can be treated as another first-order all-optical ODE solver with $k_2 = 0.032/\text{ps}$ when using port 5 and 6. Additionally, utilizing port 3 and 4, two cascaded microrings are working as a second-order all-optical ODE solver with the constant-coefficient given by: $a = k_1 + k_2 = 0.06/\text{ps}$, $b = k_1 k_2 = 0.000896/\text{ps}^2$. The measured spectra of each microring and the cascaded ones are illustrated in Fig. 5(c).

The experimental setup is shown in Fig. 5(d). We choose super-Gaussian pulse as the input signal. As for Fig. 5(a), employing port 1 & 2 and port 5 & 6, respectively, Microring 1 and Microring 2 are used as a first-order all-optical ODE solver correspondingly. The measured spectra and the output waveforms are depicted in Figs. 6(a)–(d), along with the theoretical results achieved by ideal filters.

When launching the input signal at port 3, the solution of Eq. (4.4) for $a = k_1 + k_2 = 0.06/\text{ps}$ and $b = k_1 k_2 = 0.000896/\text{ps}^2$ can be obtained at port 4 and vice versa. The measured spectrum and output waveform are demonstrated in Figs. 6(e), (f) along with the ideal ones, which confirm the feasibility of using cascaded microrings to solve high order all-optical ODE.

5. ALL-OPTICAL DIFFERENTIAL EQUATION SOLVER WITH CONSTANT-COEFFICIENT TUNABLE

From Section 3, we know that a microring can be a first-order ODE solver. And if we can change the Q value of the microring, we can build a constant-coefficient tunable ODE solver. So we fabricated an electrically tuned add-drop microring as shown in Fig. 7. Figs. 7(a) and (b) show the microscope

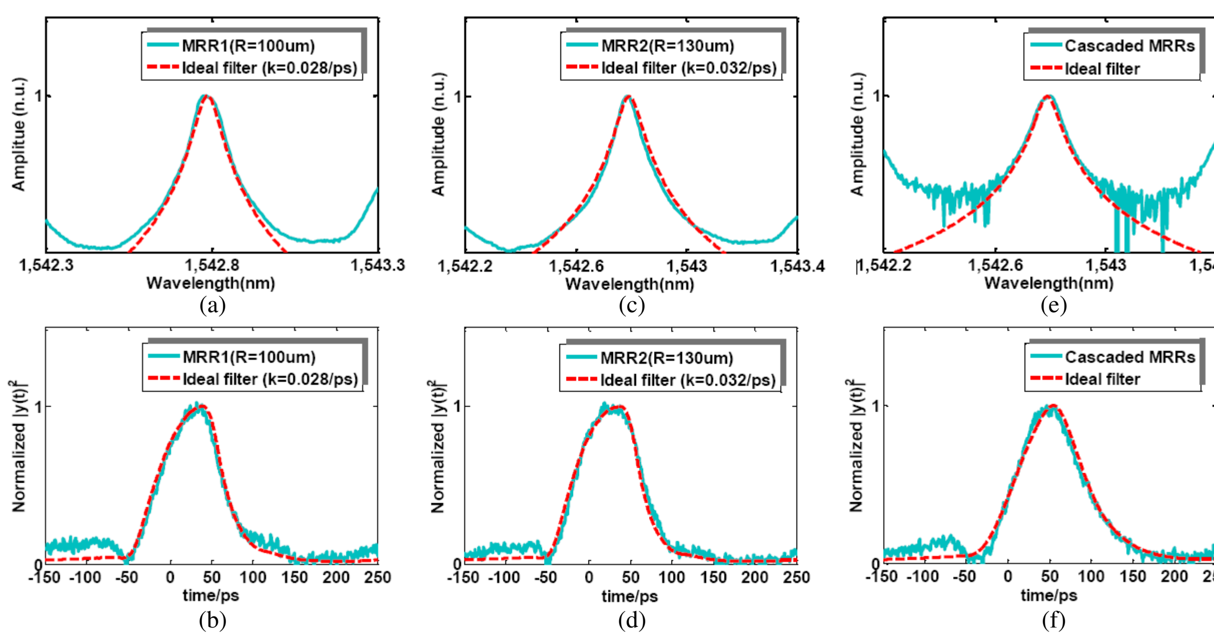

Figure 6: The plots represent both the measured experimental results (turquoise solid line) and the simulated theoretical results (red dotted line) of the spectra and temporal waveforms of the microring-based all-optical ODE solver: spectrum (a) and temporal waveform (b) for microring 1, spectrum (c) and temporal waveform (d) for microring 2, spectrum (e) and temporal waveform (f) for the cascaded microrings.

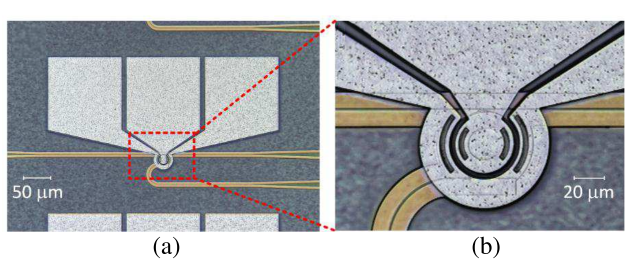

Figure 7: Microring design. (a) Microscope image of the fabricated microring, (b) microscope image of the zoom-in ring region.

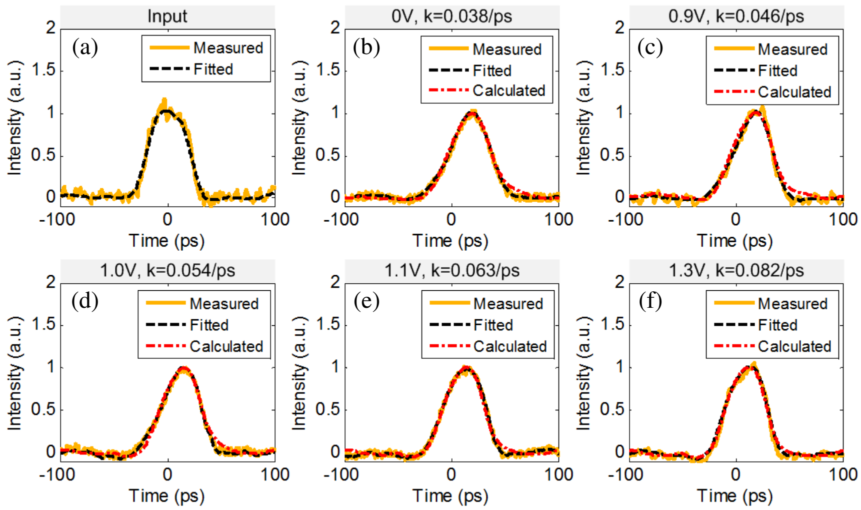

Figure 8: Experimental results for super-Gaussian input, (a) is the input waveform; yellow solid line: measured pulse, black dash line: fitted pulse, (b)–(f) are the outputs with different voltages applied on the MRR; yellow solid line: measured waveforms, black dash line: fitted waveforms and red attunement line: calculated ideal outputs.

images of the fabricated microring and the zoom-in ring region, respectively.

We choose super-Gaussian pulse as the input signal. And when the voltage applied on the microring is 0 V, corresponding to a constant-coefficient of about 0.038/ps, the output waveform (yellow solid line) is depicted in Fig. 8(b), and the calculated waveform (red attunement line) according to the ideal ODE solver is shown for comparison. When we change the voltages to 0.9 V, 1.0 V, 1.1 V and 1.3 V, corresponding to the constant-coefficient of 0.046/ps, 0.054/ps, 0.063/ps and 0.082/ps respectively, the measured output waveforms are depicted in Figs. 8(c)–(f). The fitted dash lines in Fig. 8 represent the smooth processes of measured waveforms.

6. CONCLUSION

Several schemes of ultrafast photonic differentiator and integrator was proposed and experimentally demonstrated in this paper. We demonstrated first-, second-, third-order DIFF, tunable fractional-order DIFF by on-chip MZI and first-, second-order linear ODE solver, first-order linear ODE with different values of constant-coefficient by microring. Our schemes show the advantages of compact footprint, flexible and versatile.

REFERENCES

1. Xu, J., X. L. Zhang, and J. J. Dong, "High speed all-optical differentiator based on cascading semiconductor optical amplifier and optical filter," *Opt. Lett.*, Vol. 32, No. 13, 1872–1874, 2007.
2. Xu, J., X. L. Zhang, J. J. Dong, and D. Huang, "All-optical differentiator based on cross-gain modulation in semiconductor optical amplifier," *Opt. Lett.*, Vol. 32, No. 20, 3029–3031, 2007.
3. Park, Y., M. H. Asghari, and R. Helsten, "Implementation of broadband microwave arbitrary-order time differential operators using a reconfigurable incoherent photonic processor," *IEEE Photonics Journal*, Vol. 2, No. 6, 1040–1050, 2010.
4. Velanas, P., A. Bogris, and A. Argyris, "High-speed all-optical first- and second-order differentiators based on cross-phase modulation in fibers," *Lightwave Technology*, Vol. 26, No. 18, 3269–3276, 2008.
5. Lu, L. Y., J. Y. Wu, and T. Wang, "Compact all-optical differential-equation solver based on silicon microring resonator," *Frontiers of Optoelectronics*, Vol. 5, No. 1, 99–106, 2012.
6. Tan, S. S., Z. Wu and L. Lei, "All-optical computation system for solving differential equations based on optical intensity differentiator," *Optics Express*, Vol. 21, No. 6, 7008–7013, 2013.
7. Slavík, R. Yongwoo Park, and N. Ayotte, "Photonic temporal integrator for all-optical computing," *Opt. Express*, Vol. 16, No. 22, 18202–18214, 2008.
8. Dong, J., A. Zheng, D. Gao, L. Lei, D. Huang, and X. Zhang, "Compact, flexible and versatile photonic differentiator using silicon Mach-Zehnder interferometers," *Opt. Express*, Vol. 21, No. 6, 7014–7024, 2013.